Constraints on both the symmetry energy $E_2(\rho_0)$ and its density slope $L_2(\rho_0)$ by cluster radioactivity

Niu Wan,[1] Chang Xu,[1,*] Zhongzhou Ren,[1,2] and Jie Liu[1]
[1]*School of Physics, Nanjing University, Nanjing 210093, China*
[2]*School of Physics Science and Engineering, Tongji University, Shanghai 200092, China*

(Received 5 July 2017; published 27 October 2017)

Within the density-dependent cluster model (DDCM), the decay half-lives of 22 cluster emitters are calculated by using experimental decay energies. Based on our previous study on cluster radioactivity [Phys. Rev. C **90**, 064310 (2014)], not only the quadratic symmetry energy $E_2(\rho_0)$ and its slope $L_2(\rho_0)$ but also the quartic symmetry energy $E_4(\rho_0)$ and its slope $L_4(\rho_0)$ at the saturation density ρ_0 are constrained by considering the neutron skin thicknesses in the daughter nuclei. With the extracted values of $E_2(\rho_0)$ and $L_2(\rho_0)$, the exponent γ of the quadratic density-dependent symmetry energy $E_2(\rho) = E_2(\rho_0)(\rho/\rho_0)^\gamma$ is estimated. Moreover, the symmetry energy coefficient of nuclei $a_{\text{sym}}(A)$ and the ratio κ of the surface symmetry coefficient to the volume symmetry coefficient are extracted as well.

DOI: 10.1103/PhysRevC.96.044331

I. INTRODUCTION

The nuclear equation of state (EOS) of isospin asymmetric nuclear matter has attracted much attention in both nuclear physics and astrophysics [1–5]. The energy per particle in the nuclear matter is $E(\rho,\delta) = E_0(\rho,0) + \sum_{i=2,4,\ldots} E_i(\rho)\delta^i$ with isospin asymmetry $\delta = (\rho_n - \rho_p)/(\rho_n + \rho_p)$, where $E_0(\rho,0)$ is the EOS of symmetric nuclear matter and $E_i(\rho)$ is the so-called symmetry energy of the ith order [5]. Recently, both theoretical and experimental efforts have been made to study the density dependence of the quadratic term $E_2(\rho)$ [6–12]. Around the saturation density ρ_0, $E_2(\rho)$ can be characterized by using the symmetry energy $E_2(\rho_0)$ and its density slope $L_2(\rho_0) = 3\rho\partial E_2(\rho)/\partial\rho|_{\rho=\rho_0}$: $E_2(\rho) = E_2(\rho_0) + L_2(\rho_0)\epsilon + O(\epsilon^2)$ with $\epsilon = (\rho - \rho_0)/(3\rho_0)$ [6–12]. Similarly, the quartic term $E_4(\rho)$ can be denoted as $E_4(\rho) = E_4(\rho_0) + L_4(\rho_0)\epsilon + O(\epsilon^2)$ with $L_4(\rho_0) = 3\rho\partial E_4(\rho)/\partial\rho|_{\rho=\rho_0}$. Although the value of $E_2(\rho_0)$ has been well constrained around 30 MeV [6–12], that of $L_2(\rho_0)$ is still far from high accuracy [13–24]. Danielewicz and Lee obtain a value $L_2(\rho_0) = 78-111$ MeV [15], while Centelles *et al.* suggest $L_2(\rho_0) = 75 \pm 25$ MeV [16] and $L_2(\rho_0) = 45-75$ MeV from neutron skin thicknesses of nuclei [17]. From the correlation for $E_2(\rho_0)$ and $L_2(\rho_0)$ with widely different mean-field interactions, a value $L_2(\rho_0) = 56 \pm 24$ MeV is obtained [18].

With the values of $E_2(\rho_0)$ and $L_2(\rho_0)$, the exponent of the quadratic density-dependent symmetry energy $E_2(\rho) = E_2(\rho_0)(\rho/\rho_0)^\gamma$ can be directly calculated by $\gamma = L_2(\rho_0)/[3E_2(\rho_0)]$. The property around ρ_0 has been extensively studied; however, γ retains a large uncertainty. The isospin diffusion data suggest $\gamma = 0.69-1.05$ by using an isospin-dependent Boltzmann–Uehling–Uhlenbeck (IBUU) transport model [6,7]. A value $\gamma = 0.5$ is inferred from neutron and proton transverse emission ratios [19]. Recently, to examine the density dependence of $E_2(\rho)$, a very useful tool was proposed [16] that the mass-dependent symmetry energy coefficient of nuclei $a_{\text{sym}}(A) = S_0/(1 + \kappa A^{-1/3})$ [15,25] is approximately equal to the symmetry energy $S_A = E_2(\rho_A)$ at a reference density ρ_A [16], where S_0 is the symmetry energy $E_2(\rho_0)$ at the saturation density, A is the mass number of a nucleus, and κ is the ratio of the surface symmetry coefficient to the volume symmetry coefficient [15,25]. For the nucleus ^{208}Pb, the reference density is suggested to be $\rho_A \approx 0.1$ fm^{-3} [16] and the analysis of the giant dipole resonance (GDR) in ^{208}Pb with the Skyrme interactions suggests $S_A = 23.3-24.9$ MeV [26], implying $\gamma = 0.5-0.65$ [16]. The data of the GDR in ^{132}Sn constrains it as $S_A = 21.2-22.5$ MeV [27]. From nuclear masses a value $S_A = 20.2-24.7$ MeV is extracted with $\gamma = 0.6-0.8$ [28]. With the Skyrme energy density functional, it is calculated to be $S_A = 20.8-23.6$ MeV [29], indicating $\gamma = 0.57-0.78$.

To study the density dependence of the symmetry energy $E_i(\rho)$, in our previous work [30–33], the fundamental Hugenholtz–Van Hove (HVH) theorem [34] is applied and the single-nucleon potential $U_{n/p}(\rho,\delta,k)$ is expanded as a power series in δ [30,31]. As a result, the quadratic symmetry energy $E_2(\rho_0)$ and its slope $L_2(\rho_0)$ are strictly derived to be related to the isoscalar part $U_0(\rho_0,k)$ and isovector (symmetry) part $U_{\text{sym}}(\rho_0,k)$ of the single-nucleon potential [30–33]:

$$E_2(\rho_0) = \frac{1}{6}\frac{\partial(t+U_0)}{\partial k}\bigg|_{k_F} k_F + \frac{1}{2}U_{\text{sym}}(\rho_0,k_F), \tag{1}$$

$$L_2(\rho_0) = \frac{1}{6}\frac{\partial(t+U_0)}{\partial k}\bigg|_{k_F} k_F + \frac{1}{6}\frac{\partial^2(t+U_0)}{\partial k^2}\bigg|_{k_F} k_F^2 + \frac{3}{2}U_{\text{sym}}(\rho_0,k_F) + \frac{\partial U_{\text{sym}}(\rho_0,k)}{\partial k}\bigg|_{k_F} k_F. \tag{2}$$

Based on our study in Ref. [30], the higher-order terms $(\delta^2,\delta^3,\ldots)$ of the single-nucleon potential $U_{n/p}(\rho,\delta,k)$ have very a few contributions to the symmetry energy $E_i(\rho)$. By neglecting them, the quartic symmetry energy $E_4(\rho_0)$ and its slope $L_4(\rho_0)$ can be derived to be related to $U_0(\rho_0,k)$ and

[*]cxu@nju.edu.cn

$U_{\mathrm{sym}}(\rho_0,k)$ as well:

$$E_4(\rho_0) = \frac{5}{324}\frac{\partial(t+U_0)}{\partial k}\bigg|_{k_F} k_F - \frac{1}{108}\frac{\partial^2(t+U_0)}{\partial k^2}\bigg|_{k_F} k_F^2 + \frac{1}{648}\frac{\partial^3(t+U_0)}{\partial k^3}\bigg|_{k_F} k_F^3 - \frac{1}{36}\frac{\partial U_{\mathrm{sym}}(\rho_0,k)}{\partial k}\bigg|_{k_F} k_F + \frac{1}{72}\frac{\partial^2 U_{\mathrm{sym}}(\rho_0,k)}{\partial k^2}\bigg|_{k_F} k_F^2, \tag{3}$$

$$L_4(\rho_0) = \frac{5}{324}\frac{\partial(t+U_0)}{\partial k}\bigg|_{k_F} k_F - \frac{1}{324}\frac{\partial^2(t+U_0)}{\partial k^2}\bigg|_{k_F} k_F^2 - \frac{1}{216}\frac{\partial^3(t+U_0)}{\partial k^3}\bigg|_{k_F} k_F^3 - \frac{7}{108}\frac{\partial U_{\mathrm{sym}}(\rho_0,k)}{\partial k}\bigg|_{k_F} k_F + \frac{1}{72}\frac{\partial^2 U_{\mathrm{sym}}(\rho_0,k)}{\partial k^2}\bigg|_{k_F} k_F^2 + \frac{1}{54}\frac{\partial^3 U_{\mathrm{sym}}(\rho_0,k)}{\partial k^3}\bigg|_{k_F} k_F^3. \tag{4}$$

Thus the difficult task of studying the density dependence of $E_i(\rho)$ is successfully translated into finding the single-nucleon potential, especially its symmetry part. By considering the neutron skin thickness S in the daughter nuclei of cluster and proton radioactivities, the magnitude of the symmetry potential has been extracted within the density-dependent cluster model (DDCM) [35–40] and L is constrained to be 54 ± 6 MeV [32] and 51.8 ± 7.2 MeV [33], respectively.

In this paper, to further constrain the density dependence of $E_2(\rho)$ and $E_4(\rho)$, not only the quadratic symmetry energy $E_2(\rho_0)$ and its slope $L_2(\rho_0)$ but also the quartic symmetry energy $E_4(\rho_0)$ and its slope $L_4(\rho_0)$ are extracted by 22 cluster radioactivities. With the extracted values of $E_2(\rho_0)$ and $L_2(\rho_0)$, the exponent γ is estimated as well. Besides, by applying the relationship $a_{\mathrm{sym}}(A) = S_A = E_2(\rho_A)$, the values of the mass-dependent symmetry energy coefficient of nuclei $a_{\mathrm{sym}}(A)$ and the ratio κ of the surface symmetry coefficient to the volume symmetry coefficient are both constrained.

II. CLUSTER RADIOACTIVITY STUDIED BY THE DDCM

For cluster radioactivity, the most important quantity to determine the decay half-life is the cluster penetration probability P_p [41–43]:

$$P_p = \exp\left[-2\int_{R_2}^{R_3} dR\sqrt{\frac{2\mu}{\hbar^2}|P(R)|}\right], \tag{5}$$

where R_2 and R_3 are two classical turning points and μ is the cluster-core reduced mass. The function $P(R)$ is defined as $P(R) = V(R) - Q$, where Q and $V(R)$ are the decay energy and the total cluster-core interaction, respectively. In the DDCM, $V(R)$ is usually written as a sum of nuclear potential $V_N(R)$, Coulomb potential $V_C(R)$, and centrifugal potential [41–43]:

$$V(R) = V_N(R) + V_C(R) + \frac{\hbar^2}{2\mu}\frac{\ell(\ell+1)}{R^2}, \tag{6}$$

where ℓ is the angular momentum of the cluster. The potentials $V_N(R)$ and $V_C(R)$ are obtained by the double-folded integral of the density distributions of the cluster and the core [44–46]:

$$V_N(R) = \lambda \iint d\mathbf{r}_1 d\mathbf{r}_2(\rho_{1n}+\rho_{1p})(\rho_{2n}+\rho_{2p})g_{00}(s,E), \tag{7}$$

$$V_C(R) = \iint d\mathbf{r}_1 d\mathbf{r}_2 \rho_{1p}\frac{e^2}{s}\rho_{2p}, \tag{8}$$

where $\rho_{ip/n}(r) = \rho^0_{ip/n}/\{1+\exp[(r-c_{ip/n})/a_{ip/n}]\}$ are the proton and neutron density distributions of the cluster ($i = 1$) and the core ($i = 2$) within the two-parameter Fermi (2PF) model. The half radii $c_{ip/n} = 1.07A_i^{1/3}$ fm and the diffuseness parameters $a_{ip/n} = 0.54$ fm are taken from the literature [47,48], where A_i are mass numbers. $g_{00}(s,E) = 7999\frac{\exp(-4s)}{4s} - 2134\frac{\exp(-2.5s)}{2.5s} - 276(1-0.005E/A_1)\delta(s)$ is the M3Y nucleon-nucleon interaction [45,46], and $s = |\mathbf{R}+\mathbf{r}_2-\mathbf{r}_1|$ is the distance between a nucleon in the cluster and a nucleon in the core [45,46].

In Eq. (7), the nuclear potential $V_N(R)$ of two interacting nuclei is used for overlapping nuclear fragments. In the region close to the R_2 turning point (ranging from 8.772 to 9.625 fm in the present work), nucleons of the daughter nucleus distribute diffusely and the nucleon density corresponding to the R_2 turning point is very low. Besides, as pointed out in Refs. [49,50], a cluster can only be formed in regions where the density of nuclear matter is low (approximately 1/5 of saturation density). So the large density overlap in the double folding model may not occur in this region. In the internal region, large density overlap may result in a deep nuclear potential. There are two ways in the literature to solve this problem. One is to introduce an additional repulsion potential as discussed in Refs. [51,52]. The other is to introduce a renormalization factor in the nuclear potential as discussed in Refs. [44–46]. Here we follow the second way and use a renormalization factor $\lambda = 0.55$ directly taken from Refs. [44–46] for the present calculations.

Within the two-potential approach (TPA) [53,54], the decay half-life of cluster radioactivity can be calculated by

$$T_{\mathrm{calc}} = \frac{\hbar \ln 2}{P_c F \frac{\hbar^2}{4\mu} P_p}, \tag{9}$$

where $P_c = 10^{-(0.01148 Z_1 Z_2 - 1.48585)}$ is the cluster preformation factor with Z_1 and Z_2 being the proton numbers of the cluster and the core, respectively. F is a pre-exponential factor in the decay width of modern decay theory. In nuclear textbooks, it is also known as the "frequency factor" describing the collision frequency of a cluster moving inside the parent nucleus. It is now well defined from the perspective of quantum mechanics by the TPA [53,54]. Here F is given by $F\int_{R_1}^{R_2}\frac{dR}{2|P(R)|} = 1$ where R_1 is the first turning point and $P(R) = V(R) - Q$ is given below Eq. (5).

III. CALCULATION AND DISCUSSION

In our calculations, 22 cluster radioactivities are involved and listed in the first column in Table I. The experimental decay energy Q, the angular momentum ℓ of the cluster, and

TABLE I. Calculated decay half-life $\log_{10} T_{\rm calc}$ (calc.) and the half-life difference $\Delta_T = \log_{10} T_{\rm calc} - \log_{10} T_{\rm expt}$. In the first column list the cluster radioactivities. The experimental decay energy Q, the angular momentum ℓ, and the experimental decay half-life $\log_{10} T_{\rm expt}$ (expt.) are given in the next three columns and their values are taken from Ref. [55].

Decay	Q	ℓ	Expt.	Calc.	Δ_T
${}^{221}_{87}$Fr $\to$ ${}^{207}_{81}$Tl + ${}^{14}_{6}$C	31.30	3.0	14.5	14.045	−0.455
${}^{221}_{88}$Ra $\to$ ${}^{207}_{82}$Pb + ${}^{14}_{6}$C	32.40	3.0	13.4	12.989	−0.411
${}^{222}_{88}$Ra $\to$ ${}^{208}_{82}$Pb + ${}^{14}_{6}$C	33.05	0.0	11.0	11.570	0.570
${}^{223}_{88}$Ra $\to$ ${}^{209}_{82}$Pb + ${}^{14}_{6}$C	31.85	4.0	15.2	14.041	−1.159
${}^{224}_{88}$Ra $\to$ ${}^{210}_{82}$Pb + ${}^{14}_{6}$C	30.53	0.0	15.7	16.416	0.716
${}^{226}_{88}$Ra $\to$ ${}^{212}_{82}$Pb + ${}^{14}_{6}$C	28.21	0.0	21.2	21.510	0.310
${}^{225}_{89}$Ac $\to$ ${}^{211}_{83}$Bi + ${}^{14}_{6}$C	30.48	4.0	17.2	17.850	0.650
${}^{228}_{90}$Th $\to$ ${}^{208}_{82}$Pb + ${}^{20}_{8}$O	44.72	0.0	20.7	21.414	0.714
${}^{230}_{90}$Th $\to$ ${}^{206}_{80}$Hg + ${}^{24}_{10}$Ne	57.78	0.0	24.6	24.624	0.024
${}^{231}_{91}$Pa $\to$ ${}^{207}_{81}$Tl + ${}^{24}_{10}$Ne	60.42	1.0	22.9	21.993	−0.907
${}^{232}_{92}$U $\to$ ${}^{208}_{82}$Pb + ${}^{24}_{10}$Ne	62.31	0.0	20.4	20.618	0.218
${}^{233}_{92}$U $\to$ ${}^{209}_{82}$Pb + ${}^{24}_{10}$Ne	60.51	2.0	24.8	23.306	−1.494
${}^{235}_{92}$U $\to$ ${}^{211}_{82}$Pb + ${}^{24}_{10}$Ne	57.36	1.0	27.4	28.238	0.838
${}^{233}_{92}$U $\to$ ${}^{208}_{82}$Pb + ${}^{25}_{10}$Ne	60.75	2.0	24.8	23.191	−1.609
${}^{235}_{92}$U $\to$ ${}^{210}_{82}$Pb + ${}^{25}_{10}$Ne	57.73	3.0	27.4	28.013	0.613
${}^{234}_{92}$U $\to$ ${}^{206}_{80}$Hg + ${}^{28}_{12}$Mg	74.13	0.0	25.7	25.587	−0.113
${}^{236}_{92}$U $\to$ ${}^{208}_{80}$Hg + ${}^{28}_{12}$Mg	71.83	0.0	27.6	28.761	1.161
${}^{236}_{94}$Pu $\to$ ${}^{208}_{82}$Pb + ${}^{28}_{12}$Mg	79.67	0.0	21.7	21.412	−0.288
${}^{238}_{94}$Pu $\to$ ${}^{210}_{82}$Pb + ${}^{28}_{12}$Mg	75.93	0.0	25.7	26.268	0.568
${}^{236}_{92}$U $\to$ ${}^{206}_{80}$Hg + ${}^{30}_{12}$Mg	72.48	0.0	27.6	28.201	0.601
${}^{238}_{94}$Pu $\to$ ${}^{208}_{82}$Pb + ${}^{30}_{12}$Mg	77.00	0.0	25.7	25.102	−0.598
${}^{242}_{96}$Cm $\to$ ${}^{208}_{82}$Pb + ${}^{34}_{14}$Si	96.53	0.0	23.2	23.186	−0.014

the experimental half-life $\log_{10} T_{\rm expt}$ (expt.) are in the next three columns and their values are taken from Ref. [55]. The calculated decay half-lives $\log_{10} T_{\rm calc}$ (calc.) and the half-life differences $\Delta_T = \log_{10} T_{\rm calc} - \log_{10} T_{\rm expt}$ are listed in the last two columns. The relation between the difference Δ_T and the proton number Z of the mother nucleus is shown in Fig. 1. It is clearly seen from Fig. 1 that most of the half-life differences

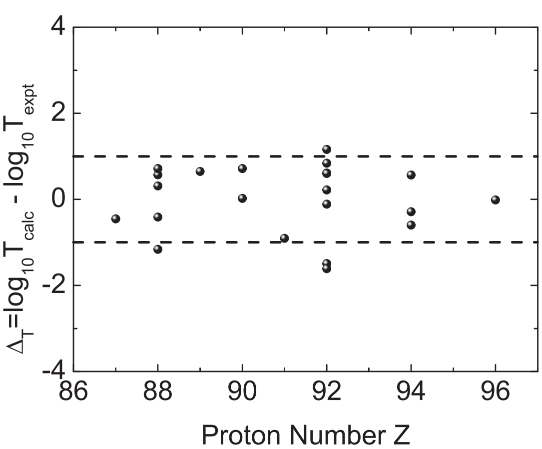

FIG. 1. Variation of the decay half-life difference Δ_T with the proton number Z of the mother nucleus.

are $|\Delta_T| < 1$ and the calculated decay half-lives agree with the experimental data.

On the other hand, if the neutron skin thickness S in the daughter nucleus is considered, the cluster-core nuclear potential consists of not only the isoscalar part $V_N(R)$ but also the isovector part $V_{\rm sym}(R)$ [32,33]. The latter is obtained from the difference between the proton and neutron density distributions [32,33]:

$$V_{\rm sym}(R) = \lambda' \int\int d\mathbf{r}_1 d\mathbf{r}_2 (\rho_{1n} - \rho_{1p})(\rho_{2n} - \rho_{2p}) g_{01}(s,E), \tag{10}$$

where λ' is the strength of $V_{\rm sym}(R)$ and $g_{01}(s,E) = -4886\frac{\exp(-4s)}{4s} + 1176\frac{\exp(-2.5s)}{2.5s} + 228(1 - 0.005E/A_1)\delta(s)$ is the isospin-dependent M3Y effective interaction [45]. By considering the symmetry potential, the decay half-life can be recalculated by [32]

$$T^S_{\rm calc} = \frac{\hbar \ln 2}{P_c F \frac{\hbar^2}{4\mu} \exp\left[-2\int_{R_2}^{R_3} dR \sqrt{\frac{2\mu}{\hbar^2}|P(R) + V_{\rm sym}(R)|}\right]}. \tag{11}$$

According to our previous studies [32,33], the strength λ' is extracted by taking $T^S_{\rm calc}/T_{\rm calc} = 1$ as a constant for each cluster radioactivity and the symmetry energies $E_{2,4}(\rho_0)$ and their slopes $L_{2,4}(\rho_0)$ can be constrained by both λ and λ'. The specific formulas are derived from Eqs. (1)–(4) as

$$E_2(\rho_0) = \frac{1}{3}\frac{\hbar^2 k_F^2}{2m}\frac{1}{1 - 1.38\lambda\rho_0 + 1.14\lambda'\rho_0\delta} + \lambda'\rho_0\left(\frac{107.215 + 92.39\lambda\rho_0}{1 - 1.38\lambda\rho_0 + 1.14\lambda'\rho_0\delta} - \frac{0.57 - 0.38\delta}{1 - 1.38\lambda\rho_0 + 1.14\lambda'\rho_0\delta}\frac{\hbar^2 k_F^2}{2m}\right), \tag{12}$$

$$L_2(\rho_0) = \frac{2}{3}\frac{\hbar^2 k_F^2}{2m}\frac{1}{1 - 1.38\lambda\rho_0 + 1.14\lambda'\rho_0\delta} + \lambda'\rho_0\left(\frac{321.645 + 277.169\lambda\rho_0}{1 - 1.38\lambda\rho_0 + 1.14\lambda'\rho_0\delta} - \frac{3.99 + 0.76\delta}{1 - 1.38\lambda\rho_0 + 1.14\lambda'\rho_0\delta}\frac{\hbar^2 k_F^2}{2m}\right), \tag{13}$$

$$E_4(\rho_0) = \left[\frac{1}{81} + \left(\frac{1}{36} + \frac{1}{81}\delta\right)1.14\lambda'\rho_0\right] \times \frac{\hbar^2 k_F^2}{2m}\frac{1}{1 - 1.38\lambda\rho_0 + 1.14\lambda'\rho_0\delta}, \tag{14}$$

$$L_4(\rho_0) = \left[\frac{2}{81} + \left(\frac{11}{108} + \frac{2}{81}\delta\right)1.14\lambda'\rho_0\right] \times \frac{\hbar^2 k_F^2}{2m}\frac{1}{1 - 1.38\lambda\rho_0 + 1.14\lambda'\rho_0\delta}, \tag{15}$$

where $\delta = \frac{N_2 - Z_2}{A_2}$ is the asymmetry of the daughter nucleus with N_2 being the neutron number. Here the effect of the asymmetry δ is also considered since $E_{2,4}(\rho_0)$ and $L_{2,4}(\rho_0)$ are constrained from different daughter nuclei. The neutron skin thicknesses S in these daughter nuclei are calculated by a linear relation to δ: $S = (0.901 \pm 0.147)\delta + (-0.034 \pm 0.023)$ fm,

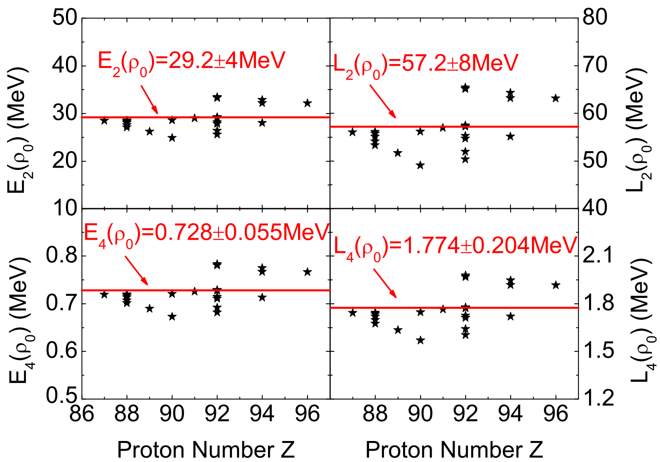

FIG. 2. Results of the symmetry energies $E_{2,4}(\rho_0)$ and their density slopes $L_{2,4}(\rho_0)$ constrained by cluster radioactivity.

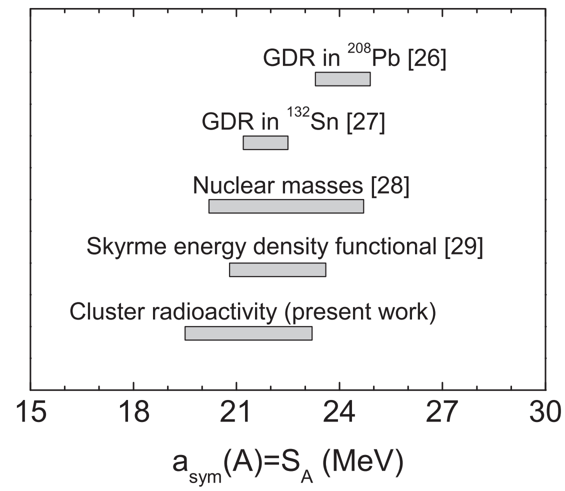

FIG. 3. Values of $a_{\rm sym}(A) = S_A = S(\rho_A)$ at the reference density $\rho_A = 0.1$ fm^{-3} for the nucleus ^{208}Pb.

which is fit by 26 neutron skin thicknesses deduced from the antiprotonic atoms [17,56,57]. Besides, as pointed in Ref. [17], the neutron skin thickness can be analytically divided into a bulk part and a surface part: $S = S^{\rm bulk} + S^{\rm surf}$, where the surface part is deduced as [17]

$$S^{\rm surf} = \sqrt{\frac{3}{5}}\frac{5\pi^2}{6}\left(\frac{a_n^2}{c_n} - \frac{a_p^2}{c_p}\right). \tag{16}$$

On the other hand, the surface part is also found to show a linear correlation to δ [17]: $S^{\rm surf} = (0.3\frac{J}{Q} + c)\delta$, where the parameters $\frac{J}{Q} = 0.667 \pm 0.047$ with $c = 0.07$ fm and $\frac{J}{Q} = 0.791 \pm 0.049$ with $c = -0.05$ fm are obtained by fitting experimental data [17]. In our calculations, the value of $S^{\rm surf}$ for each daughter nucleus is obtained from the average result of the above two sets of parameters. The constraints of the symmetry energies $E_{2,4}(\rho_0)$ and their density slopes $L_{2,4}(\rho_0)$ are shown in Fig. 2.

As shown in Fig. 2, based on the neutron skin thicknesses in the daughter nuclei of 22 different cluster radioactivities, the quadratic symmetry energy $E_2(\rho_0)$ and its density slope $L_2(\rho_0)$ are constrained and the extracted values are $E_2(\rho_0) = 29.2 \pm 4$ MeV and $L_2(\rho_0) = 57.2 \pm 8$ MeV, respectively. Meanwhile, the quartic symmetry energy $E_4(\rho_0)$ and its density slope $L_4(\rho_0)$ are respectively extracted to be $E_4(\rho_0) = 0.728 \pm 0.055$ MeV and $L_4(\rho_0) = 1.774 \pm 0.204$ MeV. These values constrained by cluster radioactivity agree very well with previous studies [17,18] and the results in Ref. [14] obtained with different approaches, indicating the reliability of our approach to some extent.

Besides, allowing for the uncertainties of the constrained quadratic symmetry energy $E_2(\rho_0)$ and its density slope $L_2(\rho_0)$, the exponent of the quadratic density-dependent symmetry energy $E_2(\rho) = E_2(\rho_0)(\rho/\rho_0)^\gamma$ is extracted to be $\gamma = 0.653^{+0.21}_{-0.16}$, which fits very well with previous studies [16,26,28,29]. Moreover, as pointed out in Ref. [16], the value of the mass-dependent symmetry energy coefficient of nuclei $a_{\rm sym}(A)$ for the nucleus ^{208}Pb can be calculated from $a_{\rm sym}(A) = S_A = E_2(\rho_A)$ at $\rho_A = 0.1$ fm^{-3}. The value is constrained to be $a_{\rm sym}(A) = S_A = 21.5^{+1.7}_{-2.0}$ MeV. Meanwhile, the ratio of the surface symmetry coefficient to the volume symmetry coefficient is extracted as $\kappa = 2.13^{+0.83}_{-0.59}$, which is also in good agreement with the values given in Refs. [28,29].

Shown in Fig. 3 are several values of the symmetry energy coefficient of nuclei $a_{\rm sym}(A) = S_A$ for the nucleus ^{208}Pb. It is clearly seen from Fig. 3 that the values of $a_{\rm sym}(A)$ extracted by the approaches applied in Refs. [26–29] are all in the range of $S_A = 20.2{-}24.9$ MeV. Except the one $S_A = 23.3{-}24.9$ MeV obtained from the GDR in ^{208}Pb [26] is relatively larger, the respective central values 21.85, 22.45, and 21.80 MeV of other three results constrained in Refs. [27–29] are consistent with each other and our value $S_A = 21.5^{+1.7}_{-2.0}$ MeV extracted by cluster radioactivity agrees with them very well.

IV. SUMMARY

In summary, following our previous study on cluster radioactivity [32], 22 cluster emitters are used in this work to further constrain the density dependence of the quadratic symmetry energy $E_2(\rho)$ and the quartic symmetry energy $E_4(\rho)$. By considering the neutron skin thicknesses in the daughter nuclei and applying the HVH theorem, not only the the quadratic symmetry energy $E_2(\rho_0)$ and its density slope $L_2(\rho_0)$ at the saturation density but also the quartic symmetry energy $E_4(\rho_0)$ and its density slope $L_4(\rho_0)$ are constrained by cluster radioactivity within the DDCM. With the constraints of $E_2(\rho_0)$ and $L_2(\rho_0)$, the exponent γ of the quadratic density-dependent symmetry energy $E_2(\rho) = E_2(\rho_0)(\rho/\rho_0)^\gamma$ is extracted. Besides, by using the relation $a_{\rm sym}(A) = S_A = E_2(\rho_A)$ at the reference density $\rho_A = 0.1$ fm^{-3} for ^{208}Pb, the value of the symmetry energy coefficient of nuclei $a_{\rm sym}(A)$ is also calculated. Moreover, the ratio κ of the surface symmetry coefficient to the volume symmetry coefficient is extracted as well and the result is in good agreement with previous studies [28,29]. Note that the present calculations can be further improved by including microscopically calculated cluster preformation factor, more realistic density distributions of the nuclei, the deformation of the emitted cluster, and so on.

ACKNOWLEDGMENTS

This work is supported by the International Science & Technology Cooperation Program of China (Grant No. 2016YFE0129300) and by the National Natural Science Foundation of China (Grants No. 11575082, No. 11535004, No. 11235001, No. 11375086, and No. 11120101005).

[1] B. A. Li, C. M. Ko, and W. Bauer, Int. J. Mod. Phys. E **07**, 147 (1998).
[2] P. Danielewicz, R. Lacey, and W. G. Lynch, Science **298**, 1592 (2002).
[3] J. M. Lattimer and M. Prakash, Science **304**, 536 (2004); Phys. Rep. **442**, 109 (2007).
[4] A. W. Steiner *et al.*, Phys. Rep. **411**, 325 (2005).
[5] B. A. Li, L. W. Chen, and C. M. Ko, Phys. Rep. **464**, 113 (2008).
[6] L. W. Chen, C. M. Ko, and B. A. Li, Phys. Rev. Lett. **94**, 032701 (2005); Phys. Rev. C **72**, 064309 (2005).
[7] D. V. Shetty, S. J. Yennello, and G. A. Souliotis, Phys. Rev. C **76**, 024606 (2007).
[8] M. B. Tsang, Y. Zhang, P. Danielewicz, M. Famiano, Z. Li, W. G. Lynch, and A. W. Steiner, Phys. Rev. Lett. **102**, 122701 (2009).
[9] Y. X. Zhang, D. D. S. Coupland, P. Danielewicz, Z. X. Li, H. Liu, F. Lu, W. G. Lynch, and M. B. Tsang, Phys. Rev. C **85**, 024602 (2012).
[10] T. X. Liu, W. G. Lynch, R. H. Showalter, M. B. Tsang, X. D. Liu, W. P. Tan, M. J. van Goethem, G. Verde, A. Wagner, H. F. Xi, H. S. Xu, M. A. Famiano, R. T. de Souza, V. E. Viola, R. J. Charity, and L. G. Sobotka, Phys. Rev. C **86**, 024605 (2012).
[11] P. Moller, W. D. Myers, H. Sagawa, and S. Yoshida, Phys. Rev. Lett. **108**, 052501 (2012).
[12] W. J. Swiatecki, A. Trzcinska, and J. Jastrzebski, Phys. Rev. C **71**, 047301 (2005).
[13] P. Danielewicz, Nucl. Phys. A **727**, 233 (2003).
[14] L. W. Chen, B. J. Cai, C. M. Ko, B. A. Li, C. Shen, and J. Xu, Phys. Rev. C **80**, 014322 (2009).
[15] P. Danielewicz and J. Lee, Nucl. Phys. A **818**, 36 (2009).
[16] M. Centelles, X. Roca-Maza, X. Vinas, and M. Warda, Phys. Rev. Lett. **102**, 122502 (2009).
[17] M. Warda, X. Vinas, X. Roca-Maza, and M. Centelles, Phys. Rev. C **80**, 024316 (2009); **81**, 054309 (2010).
[18] J. M. Dong, W. Zuo, J. Gu, and U. Lombardo, Phys. Rev. C **85**, 034308 (2012).
[19] M. A. Famiano, T. Liu, W. G. Lynch, M. Mocko, A. M. Rogers, M. B. Tsang, M. S. Wallace, R. J. Charity, S. Komarov, D. G. Sarantites, L. G. Sobotka, and G. Verde, Phys. Rev. Lett. **97**, 052701 (2006).
[20] A. Klimkiewicz *et al.*, Phys. Rev. C **76**, 051603(R) (2007).
[21] K. Sumiyoshi and H. Toki, Astrophys. J. **422**, 700 (1994).
[22] A. Carbone, G. Colo, A. Bracco, L. G. Cao, P. F. Bortignon, F. Camera, and O. Wieland, Phys. Rev. C **81**, 041301(R) (2010).
[23] I. Vidana, A. Polls, and C. Providencia, Phys. Rev. C **84**, 062801(R) (2011).
[24] W. Nazarewicz *et al.*, Eur. Phys. J. A **50**, 20 (2014).
[25] W. D. Myers and W. J. Swiatecki, Ann. Phys. (NY) **55**, 395 (1969); **84**, 186 (1974).
[26] L. Trippa, G. Colo, and E. Vigezzi, Phys. Rev. C **77**, 061304(R) (2008).
[27] L. G. Cao and Z. Y. Ma, Chin. Phys. Lett. **25**, 1625 (2008).
[28] M. Liu, N. Wang, Z. X. Li, and F. S. Zhang, Phys. Rev. C **82**, 064306 (2010).
[29] J. M. Dong, W. Zuo, and J. Z. Gu, Phys. Rev. C **87**, 014303 (2013).
[30] C. Xu, B. A. Li, and L. W. Chen, Phys. Rev. C **82**, 054607 (2010).
[31] C. Xu, B. A. Li, L. W. Chen, and C. M. Ko, Nucl. Phys. A **865**, 1 (2011).
[32] C. Xu, Z. Ren, and J. Liu, Phys. Rev. C **90**, 064310 (2014).
[33] N. Wan, C. Xu, and Z. Ren, Phys. Rev. C **94**, 044322 (2016).
[34] N. M. Hugenholtz and L. Van Hove, Physica **24**, 363 (1958).
[35] Z. Ren, C. Xu, and Z. Wang, Phys. Rev. C **70**, 034304 (2004).
[36] C. Xu and Z. Ren, Nucl. Phys. A **753**, 174 (2005).
[37] M. Ismail, A. Y. Ellithi, M. M. Botros, and A. Abdurrahman, Phys. Rev. C **86**, 044317 (2012).
[38] Y. Ren and Z. Ren, Phys. Rev. C **85**, 044608 (2012); **89**, 064603 (2014).
[39] N. Wan, C. Xu, and Z. Ren, Phys. Rev. C **92**, 024301 (2015).
[40] C. Xu, Z. Ren, G. Ropke, P. Schuck, Y. Funaki, H. Horiuchi, A. Tohsaki, T. Yamada, and B. Zhou, Phys. Rev. C **93**, 011306(R) (2016).
[41] B. Buck, A. C. Merchant, and S. M. Perez, Phys. Rev. C **45**, 1688 (1992).
[42] S. Aberg, P. B. Semmes, and W. Nazarewicz, Phys. Rev. C **56**, 1762 (1997).
[43] A. Bohr and B. Mottelson, *Nuclear Structure* (World Scientific, Singapore, 1998).
[44] G. F. Bertsch *et al.*, Nucl. Phys. A **284**, 399 (1977).
[45] G. R. Satchler and W. G. Love, Phys. Rep. **55**, 183 (1979).
[46] A. M. Kobos *et al.*, Nucl. Phys. A **384**, 65 (1982).
[47] B. Hahn, D. G. Ravenhall, and R. Hofstadter, Phys. Rev. **101**, 1131 (1956).
[48] J. D. Walecka, *Theoretical Nuclear Physics and Subnuclear Physics* (Oxford University Press, Oxford, 1995).
[49] D. M. Brink and J. J. Castro, Nucl. Phys. A **216**, 109 (1973).
[50] H. Takemoto, M. Fukushima, S. Chiba, H. Horiuchi, Y. Akaishi, and A. Tohsaki, Phys. Rev. C **69**, 035802 (2004).
[51] Ş. Mişicu and H. Esbensen, Phys. Rev. Lett. **96**, 112701 (2006).
[52] H. Esbensen and Ş. Mişicu, Phys. Rev. C **76**, 054609 (2007).
[53] S. A. Gurvitz and G. Kalbermann, Phys. Rev. Lett. **59**, 262 (1987).
[54] S. A. Gurvitz, Phys. Rev. A **38**, 1747 (1988).
[55] D. N. Basu, Phys. Lett. B **566**, 90 (2003).
[56] A. Trzcinska, J. Jastrzebski, P. Lubinski, F. J. Hartmann, R. Schmidt, T. von Egidy, and B. Klos, Phys. Rev. Lett. **87**, 082501 (2001).
[57] J. Jastrzebski, A. Trzcinska, P. Lubinski, B. Klos, F. J. Hartmann, T. von Egidy, and S. Wycech, Int. J. Mod. Phys. E **13**, 343 (2004).